Cooperative Control of Air Flow for HVAC Systems

Shuai Liu[1,2], Yushen Long[1], Lihua Xie[1] and Alexandre M. Bayen[3]

Abstract— A dynamic pressure and variable air volume (VAV) control strategy is proposed for building heating, ventilation and air-conditioning (HVAC) systems. The strategy consists in two level control, namely, pressure loop control and temperature loop control. The pressure control loop is to make sure that the air pressure at the inlet of each room is equal to a certain value while the temperature control loop is to control the room temperature which is achieved by adjusting the VAV box so that the supply air flow rate can be varied to achieve the room setting temperature. For the pressure control loop, a cooperative control technique is applied. The two control loops are coupled. This paper will analyze the stability of the overall system and give a sufficient condition on the initial values in terms of rooms and the HVAC system parameters.

I. INTRODUCTION

In recent years, energy saving and environment protection have become increasingly important. The world's growing energy demand requires developing sustainable living plans. The largest sector of energy consumption in most of cities is buildings. Usually, a great portion of the energy consumption of buildings is attributed to HVAC systems. Due to the changes of operating environment and parameters of HVAC systems, many HVAC systems cannot work in an efficient way. Therefore, the controller design of HVAC systems is a field of increasing significance.

HVAC systems can be controlled based on either static models assuming that the environment is slowly time-varying or dynamic models for real-time control. Most of the existing work on controller design is based on static models [14], and mainly focused on developing a simplified model of cooling coils. The model parameters are determined on-line, based on commission or catalog information by linear or nonlinear least squares methods. For overall HVAC systems, [4] and [5] formulate the minimization of the total power consumption, which is mainly caused by chillers, pumps and fans, as a global optimization problem. A modified genetic algorithm was used to set the optimal operating point of each component. When we consider the dynamic property of an HVAC system, the control problem becomes more difficult. A new dynamic simulation model for air-handling unit (AHU) was developed in [2]. In the work, the parameters

can be easily determined from total fan energy measurement. Since dynamic models can handle the changing environment at different times in a day over a long period of time, a dynamic control strategy can lead to a better performance compared to a static control strategy. By using Kalman filtering, [11] presents a temperature prediction algorithm based on a simple time varying zone model. The optimal performance is achieved by applying a genetic algorithm.

Room temperature can be controlled by adjusting the cool air temperature and flow rate into a room, which is controlled by a damper. There are two temperature control strategies: pressure dependent control and pressure independent control. Pressure dependent control consists in controlling the damper, based on the room temperature. Based on the temperature difference between the room temperature and the desired one, one can adjust the air flow by controlling the VAV box. The reader can refer to [12], [15], [1], [8] and [7] for example.

Pressure independent control strategies contain two control loops. The inner loop is for temperature control which can provide the set point for outer loop based on the temperature difference. The outer loop is for air pressure control. Pressure independent control leads to better control performance. This is because a pressure dependent controller will take action when the air flow changes affect the room temperature. Therefore the response of the system suffers from a time delay. However, pressure independent control has a pressure control level which is to lock the pressure at the inlet of each room. The steady air pressure makes the air flow rate smooth. Moreover, the two level control makes the controller design more flexible.

In this paper, we consider a pressure independent control strategy. Keeping the air pressure of the room inlet is the key step to air flow control. However, when adjusting a damper, not only the air pressure at the corresponding branch changes, but the pressure at all the other branches are affected. For the pressure control loop, a cooperative control strategy is developed to adjust the damper such that the air pressure of each branch converges to a desired value. The cooperative controller can reduce the pressure differences among each room inlet while tracking the desired pressure, which makes the tracking process smoother. Moreover, the controller is working in a distributed way, which means each pressure control damper is controlled based only on the pressure information of neighbor branches. Comparing with a centralized controller, the distributed one is more reliable and has low computation costs.

[1]Shuai Liu, Lihua Xie and Yushen Long are with EXQUISITUS, Centre for E-City, School of Electrical and Electronics Engineering, Nanyang Technological University, Singapore 639798 {`lius0025,elhxie,YLONG002`} at ntu.edu.sg

[2]Shuai Liu is with SinBerBEST Program, Berkeley Education Alliance for Research in Singapore, CREATE Tower, Singapore 138602 `liushuai at ntu.edu.sg`

[3]A. M. Bayen is with the Department of Electrical Engineering and Computer Sciences, and Department of Civil and Environmental Engineering, University of California, Berkeley, CA 94720 USA `bayen at berkeley.edu`
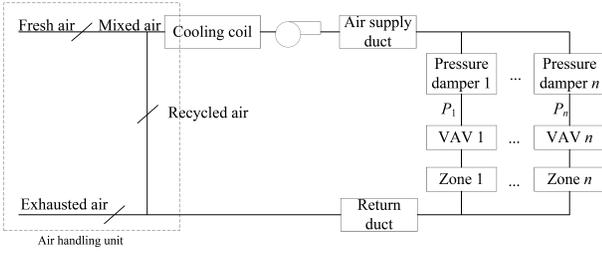
Fig. 1. Pressure-flow balance.

II. MATHEMATICAL MODEL AND PROBLEM STATEMENT

Fig.1 shows the structure of a simplified HVAC system. The left part is the AHU, which provides mixed fresh air and return air to the air supply duct. The cooling coil cools down the air provided by AHU before it is sent to the air supply duct. A fan follows which can provide positive air pressure to the air flow. Pressure control dampers are needed to control the air pressure of the corresponding branches. VAV boxes can be adjusted to change the air flow into the zones. Sometimes, a return air fan is added for better controlling the air exfiltration of the rooms. For simplicity, we do not consider the return air fan.

We assume that the room air can be mixed in no time, which means the temperature would be same everywhere in the room. The heat sources in the room are considered as constant. Under these assumptions, the room temperature can be modeled as first order system [13]

$$\dot{T}_i(t) = \dot{m}_i(t)K_{1,i}(l - T_i(t)) + K_{2,i}(s_i - T_i(t)), \quad (1)$$

where $\dot{m}_i(t)$ is the mass flow rate at the inlet of room i, T_i is the temperature in room i, l is the supplied air temperature, s_i is the temperature of heat source in room i, $K_{1,i} = \frac{\rho}{C_i}$ and $K_{2,i} = \frac{F_i}{C_i}$ are constants with C_i the room capacity, ρ the air density and F_i the specific heat capacitance. Since the dynamic pressure in the duct is negligible compared with static pressure, we consider that p_i stands for full pressure at branch duct i and the full pressure is transferred into dynamic pressure after VAV box. According to Bernoulli's equation, the mass flow rate can be expressed as

$$\dot{m}_i(t) = u_i(t)\sqrt{\frac{2P_i(t)}{\rho}}, \quad (2)$$

where u_i is the open area of the damper to be controlled in the i-th VAV box. A similar model can be found in [10].

In [3], the pressure-flow balance model is considered as an equivalent circuit system. In this paper, we consider a more general model, which is given below:

$$P_i = f_i^2(d_1, \cdots, d_n, u_i, P_{fan}), \quad (3)$$

where d_i is the opening of pressure control damper i, P_{fan} is the air pressure difference generated by the supply fan. The function f_i is nonlinear and satisfies

$$-\bar{F} \le \frac{\partial f_i}{\partial u_i} < 0, \ \frac{\partial f_i}{\partial d_j} < -\rho_1, \ i \neq j,$$

$$\sup_{j \neq i, k \neq i} \frac{\frac{\partial f_i}{\partial d_j}}{\frac{\partial f_i}{\partial d_k}} \le \gamma, \ \sum_{j=1}^n \frac{\partial f_i}{\partial d_j} > \rho_2, \quad (4)$$

where $\bar{F}$, ρ_1, ρ_2 and γ are positive constants. We assume that P_{fan} is time-invariant since the air supply fan is prevented to change its output power very often in order to maximize its lifetime and save energy. The inequalities in (4) show the coupling of the air pressure in each air duct. When the air flow resistance of pressure control damper i increases, the pressure P_i drops correspondingly. Meanwhile, the air pressure at the other inlets increases. The last inequality can be understood as that when all the pressure control dampers increase their opening, the air pressure at the inlet of each room will increase.

From (1)-(3) we can see that the temperature system and air pressure system are coupled. The objective is to control u_i such that the temperature of each room reaches its desired value. Meanwhile, the pressure is adjusted through d_i accordingly to make sure that all the pressures at the inlet of the rooms stick to a certain value, i.e.

$$\lim_{t \to \infty} T_i(t) = T_0, \ \lim_{t \to \infty} P_i(t) = P_0, \ i = 1, \ldots, n, \quad (5)$$

where T_0 and P_0 are room temperature and air pressure to be tracked. In fact, T_0 can be set as different values for different rooms. For notation convenience, we consider the case in which all rooms share a common desired temperature.

III. CONSENSUS-BASED CONTROLLER DESIGN

Most of the existing room temperature dynamic controller literature is based on PID [9], which locally controls the VAV damper i to compensate the changes of neighbors and outside environment. However, this approach does not consider the coupling of the air pressure in each air duct. When damper i is changing, the air pressure at the inlet of other rooms is affected. This may cause a bad transient response of the system. In this section, we introduce a two level control strategy, temperature control level and pressure control level. We propose a consensus-based approach for the pressure control level in order to reduce the fluctuation of air flow.

The control input of $u_i(t)$ and $d_i(t)$ are given as follows:

$$\dot{u}_i(t) = c(T_i(t) - T_0), \quad (6)$$

$$\dot{d}_i(t) = \alpha \sum_{k \in \mathcal{N}_i} \left[\left(\sqrt{P_k(t)} - \sqrt{P_i(t)} \right) + \beta \left(\sqrt{P_0} - \sqrt{P_i(t)} \right) \right], \ i = 1, \ldots, n, \quad (7)$$

where $\alpha > 0$, $\beta \ge (n-2)(\gamma - 1)$ and $c > 0$ are constants. When $\gamma = 1$, β can be chosen as any positive number. $\mathcal{N}_i$ is the set of neighboring branches that communicate their pressure information to branch i. Controller (7) is based on a widely-used distributed consensus control protocol. The dampers work in a cooperative manner. By employing cross-coupling error technology, the proposed approach can guarantee that all the pressures converge to the desired value more smoothly.

For all $i = 1, \ldots, n$, denote

$$\theta_i(t) = \sqrt{P_i(t)}, \ \tilde{\theta}_i = \theta_i - \sqrt{P_0},$$

$$\tilde{u}_i = u_i - \sqrt{\frac{\rho}{2P_0}} \frac{K_{2,i}(s_i - T_0)}{K_{1,i}(T_0 - l)}, \ x_i = \dot{\tilde{u}}_i + r_1 \tilde{u}_i,$$

$$w_{1,i} = \frac{K_{2,i}(s_i - l)}{T_0 - l}, \ w_{2,i} = \sqrt{\frac{2P_0}{\rho}} K_{1,i}(T_0 - l),$$

$$w_{3,i} = \frac{K_{2,i}(s_i - T_0)}{\sqrt{P_0}}, \ w_{12,i} = \sqrt{\frac{2P_0}{\rho}} K_{1,i},$$

$$w_{13,i} = \frac{K_{2,i}(s_i - T_0)}{\sqrt{P_0}(T_0 - l)}, \ w_{23,i} = \sqrt{\frac{2}{\rho}} K_{1,i}(T_0 - l),$$

$$w_{123,i} = \sqrt{\frac{2}{\rho}} K_{1,i},$$

$$r_1 = \frac{w_{1,i} - \sqrt{w_{1,i}^2 - 4cw_{2,i}}}{2}, \ r_2 = \frac{w_{1,i} + \sqrt{w_{1,i}^2 - 4cw_{2,i}}}{2}. \quad (8)$$

Then we have the following result.

Theorem 3.1: For the HVAC system described in Fig.1, if the initial conditions satisfy that $\forall i = 1, \ldots, n$, $\max\{|x_i(0)|, r_1|\tilde{u}_i(0)|, \frac{\rho_2}{2F}|\tilde{\theta}_i(0)|\} \in \mathcal{S}_i$, where

$$\mathcal{S}_i = \left[0, \frac{\sqrt{\phi^2 + 8w_{123,i}\left(\frac{cw_{2,i}\rho_2}{\bar{F}} - cw_{3,i}r_1\right)} - \phi}{4w_{123,i}} \right), \quad (9)$$

with $\phi = \frac{w_{12,i}\rho_2}{\bar{F}} + 2w_{13,i}r_1 + cw_{23,i}$, then all the room temperatures T_i and the static pressures P_i, $i = 1, 2, \ldots, n$ converge to T_0 and P_0 asymptotically based on the controller given in (6) and (7), where c satisfies that $\forall i = 1, \ldots, n$,

$$w_{1,i} - \sqrt{w_{1,i}^2 - 4cw_{2,i}} < \frac{2w_{2,i}\rho_2}{w_{3,i}\bar{F}}. \quad (10)$$

Proof: Denote $\tilde{T}_i = T_i - T_0$. According to (1), we have

$$\dot{\tilde{T}}_i(t) = \left[u_i(t) + \sqrt{\frac{\rho}{2P_0}} \frac{K_{2,i}(s_i - T_0)}{K_{1,i}(T_0 - l)} \right] (\sqrt{P_0} + \tilde{\theta}_i(t))$$

$$\times \sqrt{\frac{2}{\rho}} K_{1,i}(l - T_0 - \tilde{T}_i(t)) + K_{2,i}(s - T_0 - \tilde{T}_i(t))$$

$$= -w_{1,i}\tilde{T}_i(t) - w_{2,i}\tilde{u}_i(t) - w_{3,i}\tilde{\theta}_i(t)$$

$$-w_{12,i}\tilde{u}_i(t)\tilde{T}_i(t) - w_{13,i}\tilde{T}_i(t)\tilde{\theta}_i(t)$$

$$-w_{23,i}\tilde{u}_i(t)\tilde{\theta}_i(t) - w_{123,i}\tilde{u}_i(t)\tilde{T}_i(t)\tilde{\theta}_i(t), \quad (11)$$

where $w_{1,i}$, $w_{2,i}$, $w_{3,i}$, $w_{12,i}$, $w_{13,i}$, $w_{23,i}$ and $w_{123,i}$ are defined in (8). The controller (6) can be rewritten as

$$\dot{\tilde{u}}_i(t) = c\tilde{T}_i(t). \quad (12)$$

Substituting (12) into (11) yields

$$\ddot{\tilde{u}}_i(t) = -w_{1,i}\dot{\tilde{u}}_i(t) - cw_{2,i}\tilde{u}_i(t) - cw_{3,i}\tilde{\theta}_i(t)$$

$$-w_{12,i}\tilde{u}_i(t)\dot{\tilde{u}}_i(t) - w_{13,i}\dot{\tilde{u}}_i(t)\tilde{\theta}_i(t)$$

$$-cw_{23,i}\tilde{u}_i(t)\tilde{\theta}_i(t) - w_{123,i}\tilde{u}_i(t)\dot{\tilde{u}}_i(t)\tilde{\theta}_i(t). \quad (13)$$

Considering x_i as defined in (8), we can decompose (13) into the following two equations

$$\begin{cases} \dot{\tilde{u}}_i(t) = -r_1\tilde{u}_i(t) + x_i(t), \\ \dot{x}_i(t) = -r_2 x_i(t) - cw_{3,i}\tilde{\theta}_i(t) - w_{12,i}\tilde{u}_i(t)\dot{\tilde{u}}_i(t) \\ \qquad - w_{13,i}\dot{\tilde{u}}_i(t)\tilde{\theta}_i(t) - cw_{23,i}\tilde{u}_i(t)\tilde{\theta}_i(t) \\ \qquad - w_{123,i}\tilde{u}_i(t)\dot{\tilde{u}}_i(t)\tilde{\theta}_i(t), \end{cases}$$

where r_1 and r_2 are defined in (8).

According to (3), we have $\forall i = 1, 2, \ldots, n$,

$$\dot{\theta}_i(t) = \frac{\partial f_i}{\partial u_i}\dot{u}_i(t) + \sum_{j=1}^{n} \frac{\partial f_i}{\partial d_j}\dot{d}_j(t)$$

$$= \frac{\partial f_i}{\partial u_i}\dot{\tilde{u}}_i(t) + \sum_{j=1}^{n} \frac{\partial f_i}{\partial d_j}\dot{d}_j(t). \quad (14)$$

By substituting (7) into the above equation, the closed-loop system can be written into the following compact form

$$\dot{\theta}(t) = -L(t)\theta(t) + \begin{bmatrix} 0 \\ F(t)\dot{\tilde{u}}(t) \end{bmatrix}, \quad (15)$$

where $\theta = [\ \sqrt{P_0} \ \ \theta_1 \ \cdots \ \theta_n\ ]'$, $\dot{\tilde{u}} = [\ \dot{\tilde{u}}_0 \ \ \dot{\tilde{u}}_1 \ \cdots \ \dot{\tilde{u}}_n\ ]'$,

$$L(t) = \begin{bmatrix} 0 & 0 \\ b(t) & \tilde{L}(t) \end{bmatrix}, \ b(t) = \begin{bmatrix} l_{1,0} \\ \vdots \\ l_{n,0} \end{bmatrix},$$

$$\tilde{L}(t) = \begin{bmatrix} l_{1,1} & \cdots & l_{1,n} \\ \vdots & \ddots & \vdots \\ l_{n,1} & \cdots & l_{n,n} \end{bmatrix}, \ F(t) = \begin{bmatrix} \frac{\partial f_1}{\partial u_1} & & \\ & \ddots & \\ & & \frac{\partial f_n}{\partial u_n} \end{bmatrix},$$

and

$$l_{i,0}(t) = -\alpha \sum_{j=1}^{n} \frac{\partial f_i}{\partial d_j} < -\alpha\rho_2,$$

$$l_{i,i}(t) = \alpha(\beta + |\mathcal{N}_i|)\frac{\partial f_i}{\partial d_i} - \alpha \sum_{j \in \mathcal{N}i} \frac{\partial f_i}{\partial d_j} > 0,$$

$$\sup_{t \geq 0} l_{i,j}(t) = \alpha(\beta + |\mathcal{N}_i|)\frac{\partial f_i}{\partial d_j} - \alpha \sum_{k \in \mathcal{N}_j} \frac{\partial f_i}{\partial d_k} \leq 0,$$

$$j = 1, 2, \ldots, n, \ j \neq i.$$

Therefore, $L(t)$ is a valid Laplacian matrix corresponding to a leader-following graph. Since the graph is essentially connected, according to [6], P_i, $i = 1, \ldots, n$ will converge to the leader P_0 when $\dot{\tilde{u}}(t) = 0$. However, $\tilde{u}$ is time-varying and coupled with P, which makes the problem complicated. Denote $\tilde{\theta} = [\ \tilde{\theta}_1 \ \cdots \ \tilde{\theta}_n\ ]'$. Then from (15), we have

$$\dot{\tilde{\theta}}(t) = -\tilde{L}(t)\tilde{\theta}(t) + F(t)\dot{\tilde{u}}(t). \quad (16)$$

Now we define a Lyapunov function as $V(t) = \max\{\|x(t)\|_\infty, r_1\|\tilde{u}(t)\|_\infty, \frac{\rho_2}{2F}\|\tilde{\theta}(t)\|_\infty\}$. We will prove that for any $t \geq 0$, $\dot{V}(t) < 0$ almost everywhere. The proof will be discussed in the following 7 cases.

- Case 1 $(r_1\|\tilde{u}(t)\|_\infty > \max\{\|x(t)\|_\infty, \frac{\rho_2}{2F}\|\tilde{\theta}(t)\|_\infty\})$. There exists m such that $|\tilde{u}_m(t)| = \|\tilde{u}(t)\|_\infty$. According to the definition of V, it has $|r_1\tilde{u}_m(t)| > |x_m(t)|$. Then we have

$$\frac{d|\tilde{u}_m(t)|}{dt} = \text{sign}[\tilde{u}_m(t)][-r_1\tilde{u}_m(t) + x_m(t)] < 0, \quad (17)$$

which implies $\dot{V}(t) = r_1\frac{d|\tilde{u}_m(t)|}{dt} < 0$. The last inequality of (17) is because $\text{sign}[\tilde{u}_m(t)] = -\text{sign}[-r_1\tilde{u}_m(t) + x_m(t)]$.

- Case 2 ($\frac{\rho_2}{2\bar{F}}\|\tilde{\theta}(t)\|_\infty > \max\{\|x(t)\|_\infty, r_1\|\tilde{u}(t)\|_\infty\}$). There exists m such that $|\tilde{\theta}_m(t)| = \|\tilde{\theta}(t)\|_\infty$. According to the definition of V, we have

$$\left|\frac{\partial f_m}{\partial u_m}\dot{\tilde{u}}_m(t)\right| = \left|\frac{\partial f_m}{\partial u_m}(x_m(t) - r_1\tilde{u}_m(t))\right|$$
$$\leq \bar{F}|x_m(t)| + \bar{F}r_1|\tilde{u}_m(t))|$$
$$< \rho_2|\tilde{\theta}_m(t)|. \qquad (18)$$

On the other hand, according to (16) we can get the following equation

$$\dot{\tilde{\theta}}_m(t) = l_{i,0}(t)\tilde{\theta}_m(t) - \sum_{j=1}^{n} l_{i,j}(t)(\tilde{\theta}_j(t) - \tilde{\theta}_m(t))$$
$$+ \frac{\partial f_m}{\partial u_m}\tilde{u}_m(t). \qquad (19)$$

By considering (18), $l_{i,0}(t) < -\rho_2$ and $|\tilde{\theta}_j(t)| \leq |\tilde{\theta}_m(t)|$, $\sup_{t\geq 0} l_{i,j}(t) < 0$, $j = 1, \ldots, n$, we arrive at that $\text{sign}[\dot{\tilde{\theta}}_m(t)] = -\text{sign}[\tilde{\theta}_m(t)]$ and $\frac{d|\tilde{\theta}_m(t)|}{dt} < 0$, which implies $\dot{V} < 0$.

- Case 3 ($\|x(t)\|_\infty > \max\{r_1\|\tilde{u}(t)\|_\infty, \frac{\rho_2}{2\bar{F}}\|\tilde{\theta}(t)\|_\infty\}$). There exists m such that $|x_m(t)| = \|x(t)\|_\infty$. It has

$$|\tilde{\theta}_m(t)| < \frac{2\bar{F}}{\rho_2}|x_m(t)|, \ |\tilde{u}_m(t)| < \frac{|x_m(t)|}{r_1},$$
$$|\dot{\tilde{u}}_m(t)| = |-r_1\tilde{u}_m(t) + x_m(t)| < 2|x_m(t)|. \quad (20)$$

Then we have

$$\left|cw_{3,m}\tilde{\theta}_m(t) + w_{12,m}\tilde{u}_m(t)\dot{\tilde{u}}_m(t)\right.$$
$$+ w_{13,m}\dot{\tilde{u}}_m(t)\tilde{\theta}_m(t) + cw_{23,m}\tilde{u}_m(t)\tilde{\theta}_m(t)$$
$$\left.+ w_{123,m}\tilde{u}_m(t)\dot{\tilde{u}}_m(t)\tilde{\theta}_m(t)\right|$$
$$< cw_{3,m}\frac{2\bar{F}}{\rho_2}|x_m(t)| + 2w_{12,m}\frac{|x_m(t)|^2}{r_1}$$
$$+ 2w_{13,m}\frac{2\bar{F}}{\rho_2}|x_m(t)|^2 + cw_{23,m}\frac{2\bar{F}|x_m(t)|^2}{r_1\rho_2}$$
$$+ 2w_{123,m}\frac{2\bar{F}|x_m(t)|^3}{r_1\rho_2}$$
$$< r_2|x_m(t)|, \qquad (21)$$

which implies $\text{sign}[\dot{x}_m(t)] = -\text{sign}[x_m(t)]$ and therefore $\dot{V} < 0$.

- Case 4 ($\|x(t)\|_\infty = r_1\|\tilde{u}(t)\|_\infty > \frac{\rho_2}{2\bar{F}}\|\tilde{\theta}(t)\|_\infty$). There exist m and m' such that $|x_m(t)| = \|x(t)\|_\infty$ and $|\tilde{u}_{m'}(t)| = \|\tilde{u}(t)\|_\infty$. If $m \neq m'$, the proof will be the same as for Case 1 and 3. If $m = m'$, we have either $x_m(t) = r_1\tilde{u}_m(t)$ or $x_m(t) = -r_1\tilde{u}_m(t)$. When $x_m(t) = r_1\tilde{u}_m(t)$, it has $\dot{\tilde{u}}_m(t) = 0$ and $\dot{x}_m(t) < 0$. Then for any arbitrarily small number $\varepsilon > 0$, we have $|x_m(t + \varepsilon)| < |r_1\tilde{u}_m(t + \varepsilon)|$, which is Case 1. When $x_m(t) = -r_1\tilde{u}_m(t)$, it has $\text{sign}[\dot{\tilde{u}}_m(t)] = -\text{sign}[\tilde{u}_m(t)]$ and $\text{sign}[\dot{x}_m(t)] = -\text{sign}[x_m(t)]$, which implies $\dot{V} < 0$.

- Case 5 ($r_1\|\tilde{u}(t)\|_\infty = \frac{\rho_2}{2\bar{F}}\|\tilde{\theta}(t)\|_\infty > \|x(t)\|_\infty$). Assume that $|\tilde{u}_m(t)| = \|\tilde{u}(t)\|_\infty$ and $|\tilde{\theta}_{m'}(t)| = \|\tilde{\theta}(t)\|_\infty$. Similar to Case 4, we only consider $m = m'$. Since $|x_m(t)| < r_1|\tilde{u}_m(t)|$ and $|x_m(t)| < \frac{\rho_2}{2\bar{F}}|\tilde{\theta}_m(t)|$, it is

easy to prove that $\text{sign}[\dot{\tilde{u}}_m(t)] = -\text{sign}[\tilde{u}_m(t)]$ and $\text{sign}[\dot{\tilde{\theta}}_m(t)] = -\text{sign}[\tilde{\theta}_m(t)]$, which leads to $\frac{d\|\tilde{u}(t)\|_\infty}{dt} < 0$ and $\frac{d\|\tilde{\theta}(t)\|_\infty}{dt} < 0$. Then $\dot{V} < 0$ follows directly.

- Case 6 ($\|x(t)\|_\infty = \frac{\rho_2}{2\bar{F}}\|\tilde{\theta}(t)\|_\infty > r_1\|\tilde{u}(t)\|_\infty$). Since $r_1\|\tilde{u}(t)\|_\infty < \|x(t)\|_\infty$ and $r_1\|\tilde{u}(t)\|_\infty < \frac{\rho_2}{2\bar{F}}\|\tilde{\theta}(t)\|_\infty$, similar to Case 5, we can get $\frac{d\|x(t)\|_\infty}{dt} < 0$ and $\frac{d\|\tilde{u}(t)\|_\infty}{dt} < 0$, which leads to $\dot{V} < 0$.

- Case 7 ($\|x(t)\|_\infty = r_1\|\tilde{u}(t)\|_\infty = \frac{\rho_2}{2\bar{F}}\|\tilde{\theta}(t)\|_\infty > 0$). Assume that $|x_m(t)| = \|x(t)\|_\infty$, $|\tilde{u}_{m'}(t)| = \|\tilde{u}(t)\|_\infty$ and $|\tilde{\theta}_{m''}(t)| = \|\tilde{\theta}(t)\|_\infty$. We only consider $m = m' = m''$ as other cases can be considered in Case 1-6. When $x_m(t) = r_1\tilde{u}_m(t) = \frac{\rho_2}{2\bar{F}}\tilde{\theta}_m(t)$ or $x_m(t) = r_1\tilde{u}_m(t) = -\frac{\rho_2}{2\bar{F}}\tilde{\theta}_m(t)$, it has $\frac{d\|x(t)\|_\infty}{dt} < 0$, $\frac{d\|\tilde{u}(t)\|_\infty}{dt} = 0$ and $\frac{d\|\tilde{\theta}(t)\|_\infty}{dt} < 0$. Then for any arbitrarily small number $\varepsilon > 0$, we have $|x_m(t + \varepsilon)| < |r_1\tilde{u}_m(t + \varepsilon)|$ and $|\frac{\rho_2}{2\bar{F}}\tilde{\theta}_m(t)| < |r_1\tilde{u}_m(t + \varepsilon)|$, which becomes Case 1. When $x_m(t) = -r_1\tilde{u}_m(t) = \frac{\rho_2}{2\bar{F}}\tilde{\theta}_m(t)$ or $x_m(t) = -r_1\tilde{u}_m(t) = -\frac{\rho_2}{2\bar{F}}\tilde{\theta}_m(t)$, it is easy to prove that $\frac{d\|x(t)\|_\infty}{dt} < 0$, $\frac{d\|\tilde{u}(t)\|_\infty}{dt} < 0$ and $\frac{d\|\tilde{\theta}(t)\|_\infty}{dt} < 0$, which leads to $\dot{V} < 0$.

From the above cases, we conclude that $\dot{V} = 0$ only happens at denumerable time instances (in Case 4 and 7) with zero measure. It implies that $\lim_{t\to\infty} \dot{V}(t) = 0$. Then, for any arbitrarily small number $\varepsilon > 0$, there must exist a time instant t_ε such that $\forall t \geq t_\varepsilon$, $-\varepsilon < \dot{V}(t) \leq 0$. For any t satisfying $t \geq t_\varepsilon$, we consider the case in which $V(t) = r_1\|\tilde{u}(t)\|_\infty \geq \max\{\|x(t)\|_\infty, \frac{\rho_2}{2\bar{F}}\|\tilde{\theta}(t)\|_\infty\}$. The other two cases $\|x(t)\|_\infty \geq \max\{r_1\|\tilde{u}(t)\|_\infty, \frac{\rho_2}{2\bar{F}}\|\tilde{\theta}(t)\|_\infty\}$ and $\frac{\rho_2}{2\bar{F}}\|\tilde{\theta}(t)\|_\infty \geq \max\{r_1\|\tilde{u}(t)\|_\infty, \|x(t)\|_\infty\}$ can be analyzed in a similar way and will be omitted here. Assume that $|\tilde{u}_m(t)| = \|\tilde{u}(t)\|_\infty$. Since $-\varepsilon < \dot{V}(t) \leq 0$, we have

$$r_1\frac{d|\tilde{u}_m(t)|}{dt} = r_1\text{sign}[\tilde{u}_m(t)]\dot{\tilde{u}}_m(t)$$
$$= -r_1|r_1\tilde{u}_m(t) - x_m(t)| > -\varepsilon, \quad (22)$$

which implies $r_1|\tilde{u}_m(t)| - \frac{\varepsilon}{r_1} < |x_m(t)| \leq r_1|\tilde{u}_m(t)|$. On the other hand, $\dot{V} \leq 0$ implies that $|x_m(t)| \in \mathcal{S}_i$. For all $|x_m(t)| \in \mathcal{S}_i$, we can always find $\varepsilon_1 > 0$, $\Delta > 0$ and $\delta > 0$ such that $\forall \varepsilon \in (0, \varepsilon_1]$, $\forall \tau \in [t, t + \Delta)$, $|\dot{x}_m(\tau)| > \delta|x_m(\tau)|$, $\text{sign}[\dot{x}_m(\tau)] = -\text{sign}[x_m(\tau)]$ and $r_1|\tilde{u}_m(\tau)| - \frac{\varepsilon}{r_1} < |x_m(\tau)| \leq r_1|\tilde{u}_m(\tau)|$. Then we have

$$|x_m(t + \Delta)| < e^{-\delta\Delta}|x_m(t)| \leq e^{-\delta\Delta}r_1|\tilde{u}_m(t)|, \quad (23)$$

and

$$|x_m(t + \Delta)| > r_1|\tilde{u}_m(t + \Delta)| - \frac{\varepsilon}{r_1} > e^{-\varepsilon\Delta}r_1|\tilde{u}_m(t)| - \frac{\varepsilon}{r_1}. \quad (24)$$

Choose ε such that $\varepsilon < \min\{\varepsilon_1, \delta\}$. By combining (23) and (24) we have

$$V(t) = r_1|\tilde{u}_m(t)| < \frac{\varepsilon}{r_1(e^{-\varepsilon\Delta} - e^{-\delta\Delta})}.$$

The arbitrariness of ε implies that $\lim_{t\to\infty} V(t) = 0$. According to the definition of $V(t)$, it has

$$\lim_{t\to\infty} x_i(t) = 0, \ \lim_{t\to\infty} \tilde{u}_i(t) = 0, \ \lim_{t\to\infty} \tilde{\theta}_i(t) = 0,$$

which implies $\lim_{t\to\infty} P_i(t) = P_0$. Moreover, in light of (6) and (14), we have

$$\lim_{t\to\infty} (T_i(t) - T_0) = \lim_{t\to\infty} \frac{\dot{u}_i(t)}{c} = \lim_{t\to\infty} \frac{\dot{\tilde{u}}_i(t)}{c}$$
$$= \lim_{t\to\infty} \frac{x_i(t) - r_1\tilde{u}_i(t)}{c} = 0, \quad (25)$$

which completes the proof. ∎

Remark 3.1: The controller for pressure control damper is simple as shown in (7) and is easy to be implemented based on the air pressure measurements. On the other hand, the VAV box is adjusted to control the temperature. As the pressure control and temperature control are coupled. The stability of the system is analyzed in Theorem 3.1. The pressure of each branch will asymptotically converge to a common value. Meanwhile, the temperature for each zone will also asymptotically converge to the desired value. The coefficient c and α could be chosen according to the control purpose. The larger value we choose for c and α, the faster the convergence rate we can get and the larger overshoot the system will generate.

Remark 3.2: The pressure controller in (7) is designed in a cooperative manner. A damper controller is given based on the other branches pressure information named neighbor information. Once a sudden change happens in the pressure of one branch, the dampers of its neighbor branches can help to compensate the change and work in a cooperative way. The total air flow fluctuation can therefore be reduced.

IV. NUMERICAL EXAMPLE

We consider the HVAC systems with 5 rooms. The setpoint for P_i, $i = 1, \ldots, 5$ is $P_0 = 10.6 \times 10^4$ Pa. The setpoint for room temperature is $22°$C. We use MATLAB to simulate the system progress.

For the VAV damper and pressure control damper, the initial values of controller u_i and d_i, $i = 1, \ldots, 5$ are 0. The coefficients $K_{1,i}$ and $K_{2,i}$ are 0.008. We choose the coefficient c involved in (6) as 0.004, α is 0.01 and β is 1 for cooperative control. A cooling load is added in room 3 at time instant $t = 100$. Fig.2 shows the trajectories of temperature T_i under our cooperative control law, $i = 1, \ldots, 5$. For comparison, we also introduce noncooperative control law which is (7) by removing the cross-coupling error $\sqrt{P_k(t) - P_i(t)}$. Fig. 3 shows the temperature trajectories of the 5 rooms. From Fig.2 and Fig.3 we can see that the overshoot and settling time is smaller under cooperative controller. Moreover, it can be seen that all the room temperatures are keeping closer under cooperative controller. This is because the cross-coupling error term makes all the other pressure dampers close a bit after $t = 100$ to compensate the sudden pressure drop and to save the cooling air flow.

The trajectories of pressure P_i under both cooperative control and noncooperative control are given in Fig.4 and Fig.5. The trajectory of total cool air mass flow rate are compared in Fig.6. For simplicity, here we only compare the energy consumption of fan power. The energy consumption is proportional to $\int (\sum_{i=1}^5 \dot{m}_i(t))^3 dt$. To show
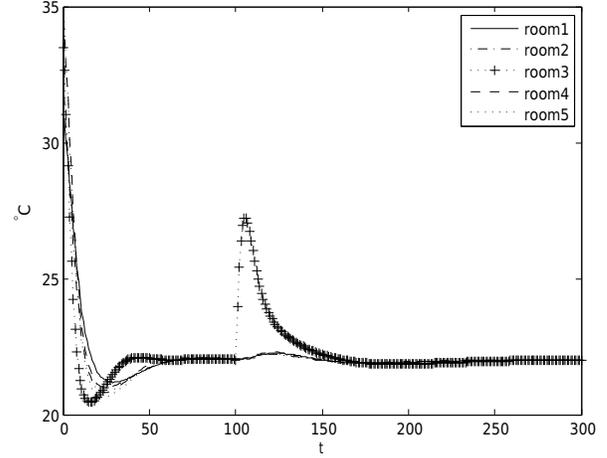

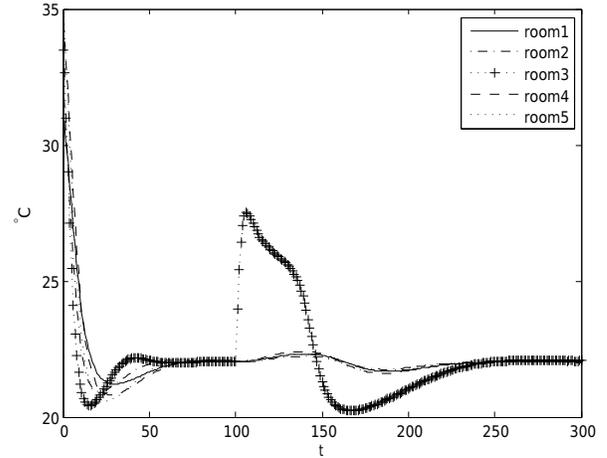Fig. 2. Temperature under cooperative control.

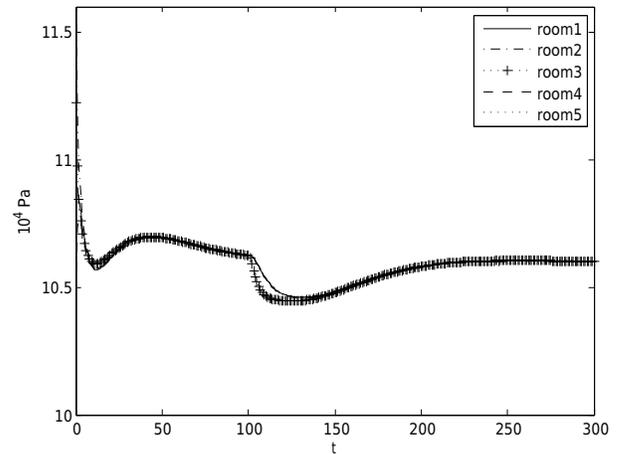Fig. 3. Temperature under noncooperative control.

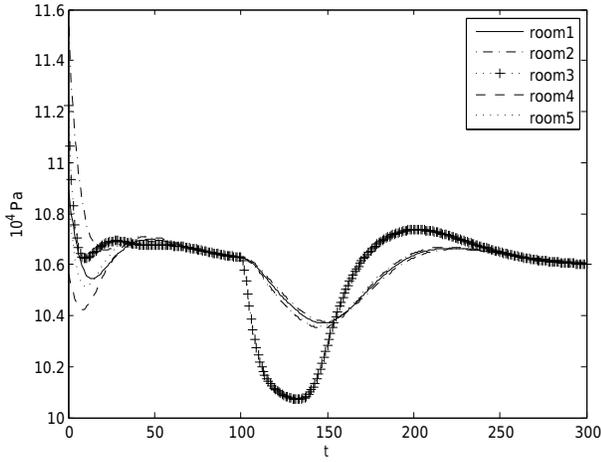Fig. 4. Air pressure of room inlets under cooperative control.

426

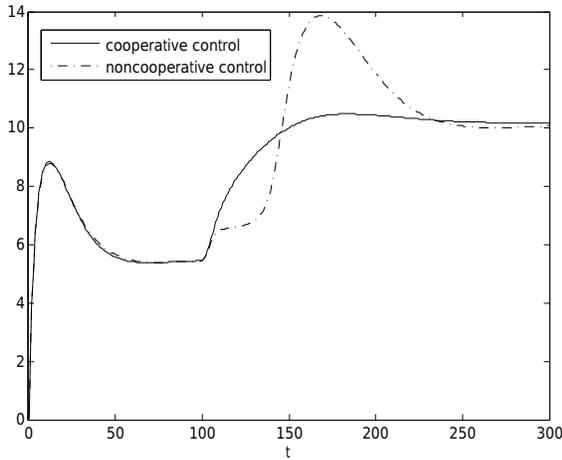Fig. 5.   Air pressure of room inlets under noncooperative control.

Fig. 6.   Cool air mass flow rate under two control laws.

the energy saving for the proposed control law, we only consider the energy consumption from $t = 100$ to the end. Under the cooperative control law (6)-(7), we have $\int_{100}^{250}(\sum_{i=1}^{5}\dot{m}_i(t))^3 dt = 1.95 \times 10^5$.

While, the energy consumption under noncooperative control law is $\int_{100}^{250}(\sum_{i=1}^{5}\dot{m}_i(t))^3 dt = 2.46 \times 10^5$, which implies 20.73% energy saving for cooperative control.

V. Conclusion

In this paper, we have considered air pressure and temperature control for HVAC systems. The VAV is controlled to guarantee that the room temperature converges to a desired value T_0. On the other hand, the pressure control damper is adjusted such that the air pressure at the inlet of the room converges to P_0. Since the air pressure is affected by the VAV boxed as well as the pressure control dampers of the neighbor branches, the systems are highly coupled. A cooperative control strategy was proposed for the pressure control dampers. The numerical examples show that the fluctuation of the total cooling air mass flow rate is reduced under the cooperative control strategy.

References

[1] R. Z. Freire, G. H. C. Oliveira, and N. Mendes, "Predictive controllers for thermal comfort optimization and energy savings," *Energy and Buildings*, vol. 40, no. 7, pp. 1353–1365, 2008.

[2] S. Li and J. Wen, "Development and validation of a dynamic air handling unit model, part 1," *ASHRAE Transactions*, vol. 116, no. 1, p. 45, 2010.

[3] S. Liu, L. Xie, and W. Cai, "Cooperative control of VAV air-conditioning systems," in *Proceedings of the 31st Chinese Control Conference*, Hefei, 2012, pp. 6938–6942.

[4] L. Lu, W. Cai, Y. S. Chai, and L. Xie, "Global optimization for overall HVAC systems-part I problem formulation and analysis," *Energy Conversion and Management*, vol. 46, no. 7-8, pp. 999–1014, 2005.

[5] L. Lu, W. Cai, Y. C. Soh, and L. Xie, "Global optimization for overall HVAC systems-part II problem solution and simulations," *Energy Conversion and Management*, vol. 46, no. 7-8, pp. 1015–1028, 2005.

[6] L. Moreau, "Stability of multiagent systems with time-dependent communication links," *IEEE Transactions on Automatic Control*, vol. 50, no. 2, pp. 169–182, 2005.

[7] P.-D. Morosan, R. Bourdais, D. Dumur, and J. Buisson, "Building temperature regulation using a distributed model predictive control," *Energy and Buildings*, vol. 42, no. 9, pp. 1445–1452, 2010.

[8] M. Mossolly, K. Ghali, and N. Ghaddar, "Optimal control strategy for a multi-zone air conditioning system using a genetic algorithm," *Energy*, vol. 34, no. 1, pp. 58–66, 2009.

[9] D. S. Naidu and C. G. Rieger, "Advanced control strategies for heating, ventilation, air-conditioning, and refrigeration systems-an overview: Part I: Hard control," *HVAC&R Research*, vol. 17, no. 1, pp. 2–21, 2011.

[10] E. L. Olsen and Q. Chen, "Energy consumption and comfort analysis for different low-energy cooling systems in a mild climate," *Energy and Buildings*, vol. 35, no. 6, pp. 560–571, 2003.

[11] G. Platt, J. Li, R. Li, G. Poulton, G. James, and J. Wall, "Adaptive HVAC zone modeling for sustainable buildings," *Energy and Buildings*, vol. 42, no. 4, pp. 412–421, 2011.

[12] R. E. Rink and N. Li, "Aggregation/disaggregation method for optimal control of multizone HVAC systems," *Energy Conversion and Management*, vol. 36, no. 2, pp. 79–86, 1995.

[13] M. Wallace, R. McBride, S. Aumi, P. Mhaskar, J. House, and T. Salsbury, "Energy efficient model predictive building temperature control," *Chemical Engineering Science*, vol. 69, no. 1, pp. 45–58, 2012.

[14] Y.-W. Wang, W.-J. Cai, Y.-C. Soh, S.-J. Li, L. Lu, and L. Xie, "A simplified modeling of cooling coils for control and optimization of HVAC systems," *Energy Conversion and Management*, vol. 45, no. 18-19, pp. 2915–2930, 2004.

[15] G. R. Zheng and M. Zaheer-Uddin, "Optimization of thermal processes in a variable air volume HVAC system," *Energy*, vol. 21, no. 5, pp. 407–420, 1996.